Enhanced Charge-Carrier Mobility Derived from Cyclization of a Silanylene Unit on Dithienosiloles: Syntheses, Photophysical Properties, and Device Fabrication of Dithieno-spiro-siloles

Ho-Jin Son, Won-Sik Han, Ji-Yun Chun, Soon-Nam Kwon, Jaejung Ko,* and Sang Ook Kang*

Department of Materials Chemistry, Korea University, 208 Seochang, Chochiwon, Chung-nam 339-700, South Korea

Received December 3, 2007

A series of trimethylsilyl-substituted dithieno-spiro-siloles (**3**), with a four- to six-membered silacycloalkyl substituent at the 1,1-position, were prepared by reacting 3,3′-dilithio-5,5′-bis(trimethylsilyl)-2,2′-dithiophene (**2**) with the corresponding silacycloalkyl dichlorosilane precursors (**1**). Arylamino-substituted bis(diarylamino)dithieno-spiro-siloles (**6**) were also prepared using the same synthetic protocol by reacting 3,3′-dilithio-5,5′-bis(diarylamino)-2,2′-dithiophene (**5**) with **1**. A structural study of the five-membered dithieno-spiro-silole, 1,1-(silacyclopentenyl)dithieno-spiro-silole (**3b**), was undertaken and showed a reduced intermolecular distance in the solid state. This resulted in enhanced charge-carrier mobility, which was confirmed by a time-of-flight (TOF) measurement of **6b**. The electronic properties of dithienosiloles (**6**) were studied for device fabrication by applying them as emitting materials in multilayer devices. Thus, $I-V$ characteristics of multilayer devices, comprising *N,N*′-bis(1-naphthyl)-*N,N*′-diphenylbenzidine (NPB) as the hole-transport layer, **6** as the emitting layer, 2,9-dimethyl-4,7-diphenylphenanthroline (BCP) as the hole-blocking layer, and tris(8-quinolinato)aluminum (Alq_3) as the electron-transporting layer, showed that the dithieno-spiro-siloles (**6b**−**d**) exhibited turn-on voltages (2.2−2.8 V) lower than those of optimized dithienosilole (**2Ph-NPB**) (4.3 V). Furthermore, systematic blue shifts in both UV and PL spectra were observed in the bis(trimethylsilyl)dithieno-spiro-silole series (**3**) as the size of the exocyclic silanylene ring was increased, whereas bis(diarylamino)dithieno-spiro-siloles (**6**) exhibited only a small variation along the series due to extensive conjugation from the peripheral diarylamine to the dithienosilole core. This blue shift is attributed to elevation of the LUMO level on the basis of a DFT calculation on **3**, along with UV spectral data and cyclic voltammograms.

Introduction

Silole-based π-conjugated compounds and their derivatives have been actively studied as promising electroluminescent materials because of their unique electronic structure, formed by $\sigma^*-\pi^*$ conjugation between the σ^* orbital of the silicon atom and the π^* orbital of the butadiene moiety.[1] In an effort to exploit the advantageous properties afforded by silole units, much attention has been directed toward extended π-conjugated silole systems, especially dithienosiloles. A fused tricyclic ring system, consisting of a thiophene−silole−thiophene array, is a potential candidate for application as an electroluminescent (EL) material in organic light-emitting diodes (OLEDs)[2] and as a semiconductor in organic thin-film transistors (OTFTs).[3] Many attempts have been made to improve the EL performance of

* Corresponding author. Tel: +82-41-860-1334. Fax: +82-41-867-5396. E-mail: sangok@korea.ac.kr.

(1) (a) Chen, J.; Cao, Y. *Macromol. Rapid Commun.* **2007**, *28*, 1714. (b) Wang, F.; Wang, L.; Chen, J.; Cao, Y. *Macromol. Rapid Commun.* **2007**, *28*, 2012. (c) Yan, D.; Mohsseni-Ala, J.; Auner, N.; Bolte, M.; Bats, J. W. *Chem.−Eur. J.* **2007**, *13*, 7204. (d) Dong, Y.; Lam, J. W. Y.; Qin, A.; Li, Z.; Liu, J.; Sun, J.; Dong, Y.; Tang, B. Z. *Chem. Phys. Lett.* **2007**, *446*, 124. (e) Yu, J.; Li, W.; Jiang, Y.; Li, L. *Jpn. J. Appl. Phys.* **2007**, *46*, 31. (f) Watkins, N. J.; Makinen, A. J.; Gao, Y.; Uchida, M.; Kafafi, Z. H. *J. Appl. Phys.* **2006**, *100*, 103706. (g) Lee, S. H.; Jang, B.-B.; Kafafi, Z. H. *J. Am. Chem. Soc.* **2005**, *127*, 9071. (h) Boydston, A. J.; Yin, Y.; Pagenkopf, B. L. *J. Am. Chem. Soc.* **2004**, *126*, 3724. (i) Xu, C.; Wakamiya, A.; Yamaguchi, S. *Org. Lett.* **2004**, *6*, 3707. (j) Kim, W.; Palilis, L.; Uchida, M.; Kafafi, Z. H. *Chem. Mater.* **2004**, *16*, 4681. (k) Hissler, M.; Dyer, P. W.; Reau, R. *Coord. Chem. Rev.* **2003**, *244*, 1. (l) Roques, N.; Gerbier, P.; Sutter, J.-P.; Guionneau, P.; Luneau, D.; Guerin, C. *Organometallics* **2003**, *22*, 4833. (m) Yamaguchi, S.; Tamao, K. *J. Organomet. Chem.* **2002**, *653*, 223. (n) Losehand, U.; Mitzel, N. W. *Dalton Trans.* **2000**, 1049. (o) Tamao, K.; Yamaguchi, S. *J. Organomet. Chem.* **2000**, *611*, 5. (p) Adachi, A.; Yasuda, H.; Sanji, T.; Sakurai, H.; Okita, K. *J. Lumin.* **2000**, *87* (89), 1174. (q) Yamaguchi, S.; Jin, R.-Z.; Tamao, K. *J. Am. Chem. Soc.* **1999**, *121*, 2937. (r) Sohn, H.; Huddleston, R. R.; Powell, D. R.; West, R. *J. Am. Chem. Soc.* **1999**, *121*, 2935. (s) Sanji, T.; Sakai, T.; Kabuto, C.; Sakurai, H. *J. Am. Chem. Soc.* **1998**, *120*, 4552. (t) Yamaguchi, S.; Tamao, K. *Dalton Trans.* **1998**, 3693. (u) Yamaguchi, S.; Jin, R.-Z.; Tamao, K. *Organometallics* **1997**, *16*, 2486. (v) Tamao, K.; Yamaguchi, S.; Shiro, M. *J. Am. Chem. Soc.* **1994**, *116*, 11715. (w) Colomer, E.; Corriu, R. J. P.; Lheureux, M. *Chem. Rev.* **1990**, *90*, 265.

(2) (a) Kim, D.-H.; Ohshita, J.; Lee, K.-H.; Kunugi, Y.; Kunai, A. *Organometallics* **2006**, *25*, 1511. (b) Ohshita, J.; Hamamoto, D.; Kimura, K.; Kunai, A. *J. Organomet. Chem.* **2005**, *690*, 3027. (c) Lee, K.-H.; Ohshita, J.; Kunai, A. *Organometallics* **2004**, *23*, 5481. (d) Liu, M. S.; Luo, J.; Jen, A. K.-Y. *Chem. Mater.* **2003**, *15*, 3496. (e) Ohshita, J.; Kai, H.; Sumida, T.; Kunai, A.; Adachi, A.; Sakamaki, K.; Okita, K. *J. Organomet. Chem.* **2002**, *642*, 137. (f) Ohshita, J.; Kai, H.; Takata, A.; Iida, T.; Kunai, A.; Ohta, N.; Komaguchi, K.; Shiotani, M.; Adachi, A.; Sakamaki, K.; Okita, K. *Organometallics* **2001**, *20*, 4800. (g) Ohshita, J.; Nodono, M.; Takata, A.; Kai, H.; Adachi, A.; Sakamaki, K.; Okita, K.; Kunai, A. *Macromol. Chem. Phys.* **2000**, *201*, 851. (h) Ohshita, J.; Nodono, M.; Kai, H.; Watanabe, T.; Kunai, A.; Komaguchi, K.; Shiotani, M.; Adachi, A.; Okita, K.; Harima, Y.; Yamashita, K.; Ishikawa, M. *Organometallics* **1999**, *18*, 1453. (i) Adachi, A.; Ohshita, J.; Kunai, A.; Okita, K. *Jpn. J. Appl. Phys.* **1999**, *38*, 2148. (j) Ohshita, J.; Nodono, M.; Watanabe, T.; Ueno, Y.; Kunai, A.; Harima, Y.; Yamashita, K.; Ishikawa, M. *J. Organomet. Chem.* **1998**, *553*, 487. (k) Adachi, A.; Ohshita, J.; Kunai, A.; Kido, J.; Okita, K. *Chem. Lett.* **1998**, 1233.

(3) (a) Usta, H.; Lu, G.; Facchetti, A.; Marks, T. J. *J. Am. Chem. Soc.* **2006**, *128*, 9034. (b) Ohshita, J.; Lee, K.-H.; Hamamoto, D.; Kunugi, Y.; Ikadai, J.; Kwak, Y.-W.; Kunai, A. *Chem. Lett.* **2004**, *33*, 892.

10.1021/om7012088 CCC: $40.75
Publication on Web 05/10/2008

Chart 1. New Types of Spiro-silacycloalkyl Dithienosiloles (3 and 6)

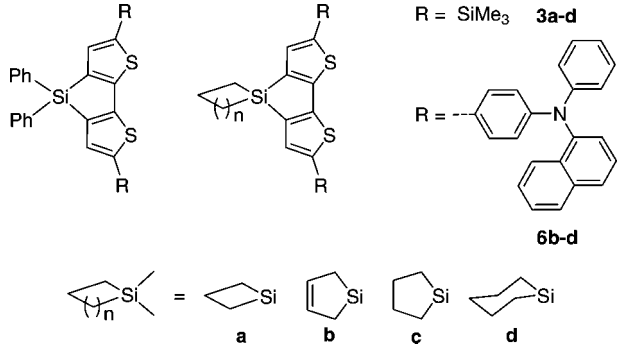

dithienosilole systems; these efforts have been focused mainly on using the electron-donating[2b,c] and -withdrawing groups[2f,4] at the α,α′-positions of bithiophene. Recently, improved EL performance was reported when bipolar character was added to the system, comprising a bis(diarylaminophenyl) unit substituted at the 5,5′-position of the dithienosiloles.[5] It has been assumed that the intermolecular distance in the solid state is related to charge-transporting capability and thereby affects the performance of the EL device.[6] Because a silole unit contains a tetrahedral silicon atom, bulky substituents such as phenyl groups on a silicon atom in a planar dithienosilole backbone need to be replaced by the less bulky substituents that could reduce the intermolecular distances in the solid state. In an effort to reduce steric packing caused by silicon substituents, cyclization on a silanylene unit in dithienosilole was proposed on the basis of our previous experiments with tetraphenyl-substituted silole derivatives.[7] Indeed, when a cyclic silanylene unit was incorporated into the dithienosilole system, enhanced charge-transport properties were observed. Thus, a series of cyclic-silanylene-substituted 5,5′-bis(trimethylsilyl)dithienosiloles (**3**) were prepared, and a structural study on the five-membered cyclic-silanylene surrogate **3b** showed that the exocyclic silacycloalkyl ring is arranged perpendicular to the dithienosilole plane. This unique conformation resulted in a reduced intermolecular distance in the solid state when compared with that found in diphenyl-substituted dithienosilole **2Ph-TMS**. This, in turn, provides a rational explanation for obtaining high EL performance from arylamino-substituted bis(diarylamino)dithienospiro-siloles (**6**).

Scheme 1. Preparation of New Types of Spiro-silacycloalkyl Dithienosiloles (3)

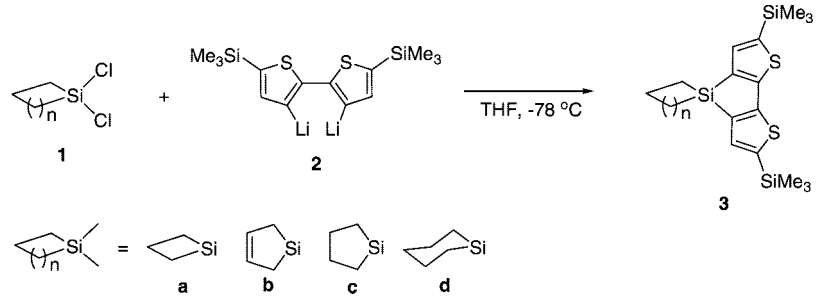

Scheme 2. Preparation of New Types of Spiro-silacycloalkyl Dithienosiloles Having a Triarylamine Unit (6)

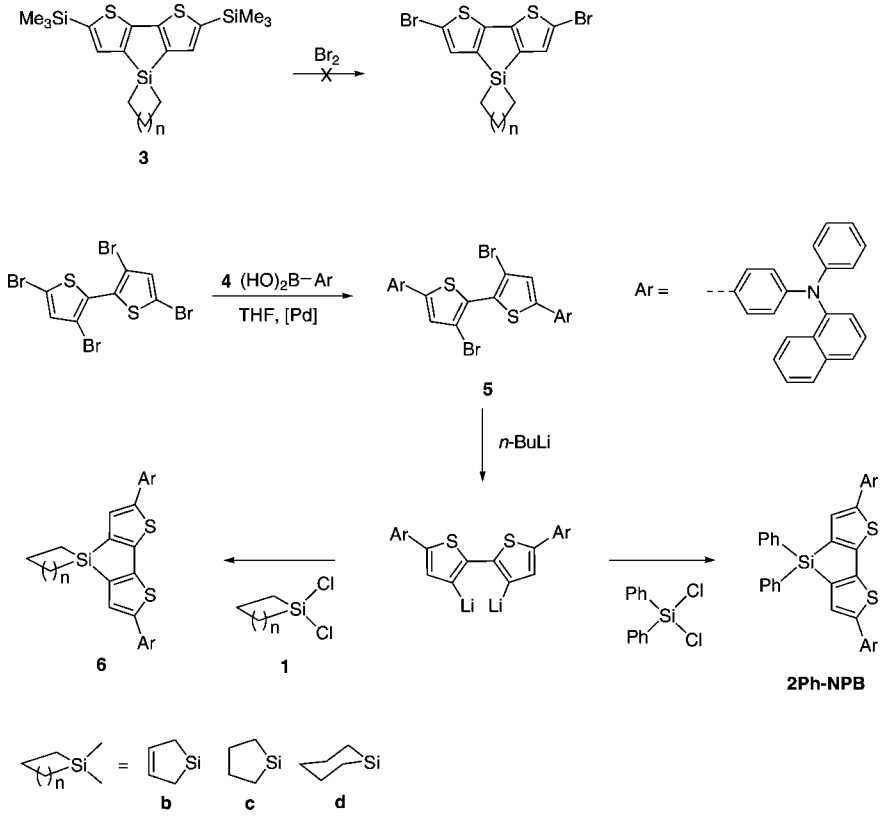

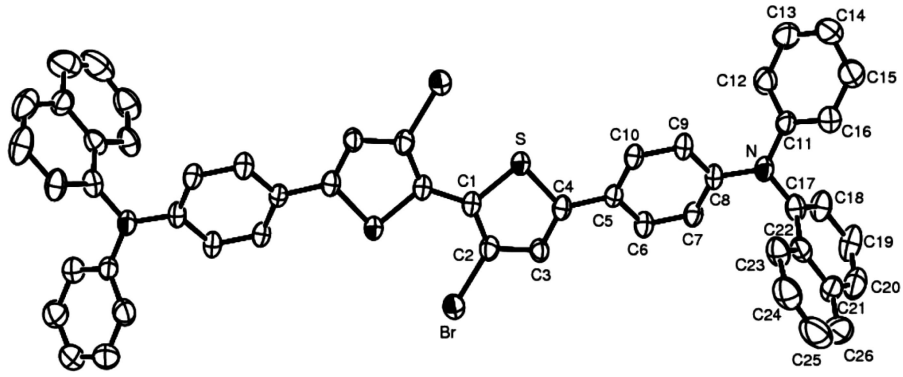

Figure 1. ORTEP drawing (30% probability thermal ellipsoids) of **5**. Hydrogen atoms and solvents are omitted for clarity.

Here, we report the full details of the syntheses and characterizations of the two series of exocyclic ring-modified dithieno-spiro-siloles, the correlation between the intermolecular interaction and the charge-carrier mobility, and finally the application of these compounds in OLEDs.

Results and Discussion

Synthesis of Exocyclic Silacycloalkyl Dithieno-spiro-siloles. Our synthesis route to 5,5′-bis(trimethylsilyl)dithieno-spiro-siloles (**3**) is shown in Scheme 1.[2h] 3,3′-Dilithio-5,5′-bis(trimethylsilyl)-2,2′-dithiophene (**2**) was prepared in situ from the reaction of 3,3′-dibromo-5,5′-bis(trimethylsilyl)-2,2′-dithiophene with *n*-butyllithium in THF. A subsequent metathesis reaction between **2** and silacycloalkyldichlorides (**1**) produced the desired silacycloalkyl dithieno-spiro-siloles (**3**) in moderate yields (47−55%).

Products were isolated by flash column chromatography, and the formation of dithieno-spiro-siloles (**3**) was confirmed by means of high-resolution mass spectrometry and elemental analyses. Bis(diarylamino)dithieno-spiro-siloles (**6**) were produced by a new route rather than the previously reported synthetic protocol.[5] As shown in Scheme 2, the treatment of **3** with 2 equiv amounts of bromine resulted in cleavage of the CySi−C bond (Cy = silacycloalkyl unit), producing 3,3′,5,5′-tetrabromobithiophene. Thus, an alternative synthetic procedure was developed utilizing the Suzuki-coupling reaction between 3,3′,5,5′-tetrabromobithiophene and 2 equiv of (*N*-1-naphthyl-*N*-phenylamino)-1-phenylboronic acid (**4**) to produce 5,5′-dibromobithiophene precursor (**5**). High-yield production (90−98%) of **5** led to the successful isolation of bis(diarylamino)dithieno-spiro-siloles (**6**), as shown in Scheme 2. However, the four-membered exocyclic surrogate **6a** was not isolated using this synthetic method due to the ring strain caused by the formation of a silacyclobutyl ring. Acyclic analogues of 1,1-diphenyl-5,5′-bis(trimethylsilyl)-2,2′-dithienosilole (**2Ph-TMS**) and 1,1-diphenyl-5,5′-bis[*N*-1-naphthyl-*N*-phenylamino)-1-phenyl]-2,2′-dithienosilole (**2Ph-NPB**) were prepared using synthetic methods similar to those employed for **3** and **6**, respectively.

All dithieno-spiro-siloles, **3** and **6**, showed the expected signals in the ^{1}H and ^{13}C NMR spectra, characteristic of exocyclic silacycloalkyl groups along with 5,5′-bis(trimethylsilyl) and bis(diarylamino) functional groups (see Experimental Section). The selective C−C bond formation was further confirmed by single-crystal X-ray structural analysis of **5** (see Figure 1).

Crystal Structure of Silole Derivatives. The solid-state structures of 1,1-(silacyclopentenyl)dithieno-spiro-silole (**3b**) and 1,1-(diphenyl)dithienosilole (**2Ph-TMS**) were confirmed by X-ray crystallographic structural studies (Figures 2 and 3). Their crystal data are summarized in Table 1, and selected bond distances and angles are listed in Table 2. Nine terminal carbon atoms (C15, C17, C18, C28, C29, C32, C33, C34, C35) for **3b** and one phenyl carbon (C13) for **2Ph-TMS** were disordered over two positions. Therefore, the site occupancies were refined using the PART instruction in SHELXL 97.[8] Exocyclic dithieno-spiro-silole (**3b**) and acyclic dithienosilole (**2Ph-TMS**) were compared in terms of bond distances and angles around the central silole unit. The two thiophene rings are almost planar, as indicated by the torsion angles at the silole sp^2 carbons. The endocyclic C−C (single) and C═C (double) bond lengths are within the range of normal single- and double-bond values (mean C−C 1.45 vs C═C 1.37 Å) found in other dithienosilole derivatives. The exocyclic Si−C bond lengths of 1.86 Å are comparable to those of endocyclic Si−C bonds. However, introduction of a cyclic ring on the silicon atom of the dithienosiloles induced reduced steric crowding at the bridgehead position of the silicon atom, as shown in Figure 2. Due to the formation of a spiro-type geometry, the exocyclic C−Si−C bond angle of **3b** is smaller than that of **2Ph-TMS** (95.8(3)° for **3b** vs 110.7(2)° for **2Ph-TMS**).

Figure 3b gives the results obtained by examining intermolecular interactions in the crystal packing. **2Ph-TMS** has CH$\cdots\pi$ interactions between a hydrogen atom of the trimethylsilyl moiety and a nearby phenyl ring at the bridgehead silicone atom. Such CH$\cdots\pi$ interactions induce an "edge-on" type molecular orientation in the crystal packing. The geometrical parameters for CH$\cdots\pi$ interactions favorably match

(4) Ohshita, J.; Lee, K.-H.; Hashimoto, M.; Kunugi, Y.; Harima, Y.; Yamashita, K.; Kunai, A. *Org. Lett.* **2002**, *4*, 1891.

(5) Lee, T.; Jung, I.; Song, K. H.; Lee, H.; Choi, J.; Lee, K.; Lee, B. J.; Pak, J. Y.; Lee, C.; Kang, S. O.; Ko, J. *Organometallics* **2004**, *23*, 5280.

(6) (a) Huby, N.; Hirsch, L.; Aubouy, L.; Gerbier, P.; Lee, A. V. D.; Amy, F.; Kahn, A. *Phys. Rev. B* **2007**, *75*, 115416. (b) Karle, I. L.; Butcher, R. J.; Wolak, M. A.; Da Silva Filho, D. A.; Uchida, M.; Bredas, J.-L.; Kafafi, Z. H. *J. Phys. Chem. C* **2007**, *111*, 9543. (c) Aubouy, L.; Gerbier, P.; Guérin, C.; Huby, N.; Hirsch, L.; Vignau, L. *Synth. Met.* **2007**, *157*, 91. (d) Yin, S.; Yi, Y.; Li, Q.; Yu, G.; Liu, Y.; Shuai, Z. *J. Phys. Chem. A* **2006**, *110*, 7138.

(7) Son, H.-J.; Han, W.-S.; Chun, J.-Y.; Lee, C.-J.; Han, J.-I.; Ko, J.; Kang, S. O. *Organometallics* **2007**, *26*, 519.

(8) Sheldrick, G. M. *SHELX97 and SHELXL97*; University of Goettingen: Germany, 1997.

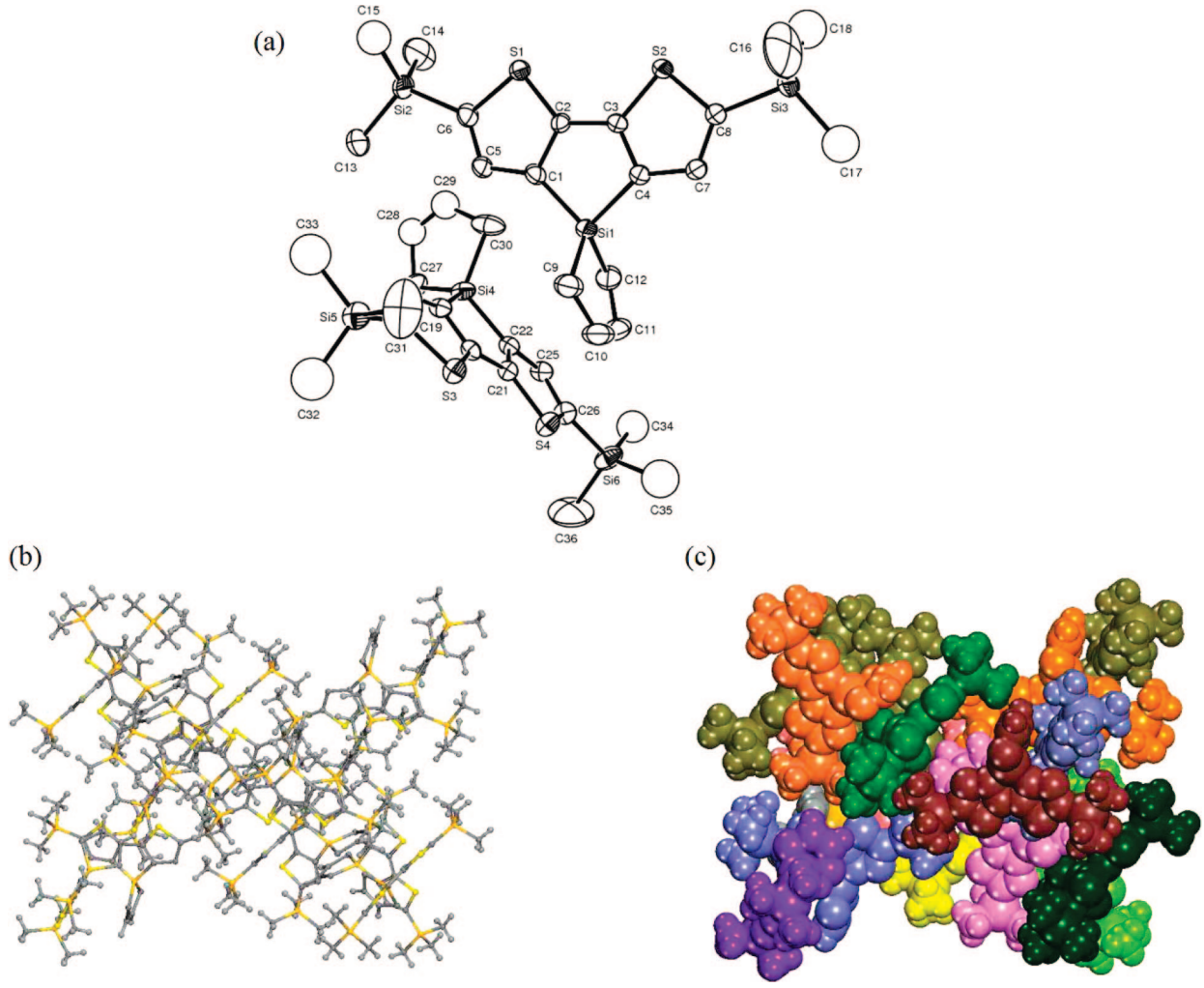

Figure 2. ORTEP drawing (30% probability thermal ellipsoids) of **3b**. Nine terminal carbon atoms (C15, C17, C18, C28, C29, C32, C33, C34, C35) in the trimethylsilyl and cyclopentenyl rings were disordered over two positions. These disordered atoms were refined isotropically to avoid unusual displacement parameters and are shown by circles in the diagram. Hydrogen atoms have been omitted for clarity. Crystal packing structure (b) and space-filling diagram (c) of **3b**.

those found in other weakly CH-π bonded systems:[9] the distances (Å) between H in donor C−H and the center of the acceptor π ring and the angles (deg) for [H in donor C−H]−[C in acceptor π ring]−[H in acceptor π ring] are estimated to be in the range 2.98−3.28 Å and 109.49−120.89°, respectively. Dithieno-spiro-silole (**3b**) consists of two perpendicular planes defined by the dithiophenosilole and silacyclopentenyl ring, which cross at the silicon atom, producing less exposure around the silicon center. A similar molecular shrinkage was observed in the case of exocyclic tetraphenylsiloles.[7] This shrinkage was further confirmed on the basis of the reduced intermolecular distance of **3b** in the crystal packing (Figure 2b). From the direct measurement of the intermolecular Si−Si distance, the intermolecular distances for **3b** and **2Ph-TMS** are 5.533 and 9.596 Å, respectively, as shown in Figure S5 and Table S1 (see Supporting Information). Thus, the intermolecular distance of **3b** is much smaller than that of **2Ph-TMS**, indicating that the perpendicular blade shape of the dithieno-spiro-silole induces a compact packing in the solid-state structure. Cyclization of the 1,1-position of the silicon atom forces the dithienosilole frame into a spiro shape, and the resulting two-face spiro conformation induces maximum intermolecular stacking in the solid state.

Photophysical Properties of Silole Derivatives. The UV−visible absorption and fluorescence spectra of the silacycloalkyl dithieno-spiro-siloles (**3** and **6**) were measured in chloroform and as solid films; the resulting spectral data are summarized in Table 3. For compounds **3**, the UV−visible absorption spectral characteristics depend on the size of the 1,1-substituted silacycloalkyl ring. In particular, increasing the size of the ring leads to a blue shift of the absorption maximum from 366 nm for **3a** to 353 nm for **3d**, as shown in Figure 4. The emission maxima also showed a similar hypsochromic shift: the wavelength of photoluminescence (PL) in the solid film showed a blue shift of about 17 nm (Figure 5). This result indicates that the electronic properties of dithieno-spiro-siloles are affected by the ring size.[7] However, it should be emphasized that with the exception of **3a** the blue shift trend of **3b**-**3d** is not apparent.

Bis(diarylamino)dithieno-spiro-siloles (**6**) exhibit band gap energies smaller than those obtained for **3** due to the long conjugation from the two triarylamine substituents. Compared

(9) (a) Karle, I. L.; Butcher, R. J.; Wolak, M. A.; da Silva Filho, D. A.; Uchida, M.; Bredas, J.-L.; Kafafi, Z. H. *J. Phys. Chem. C* **2007**, *111*, 9543. (b) Desiraju, G. R.; Steiner, T. *The Weak Hydrogen Bond in Structural Chemistry and Biology, IUCr Series*; Oxford University Press: New York, 1999; pp 140 and 191. (c) Nishio, M. *Cryst. Eng. Commun.* **2004**, *6*, 130. (d) Gulyani, A.; Srinivasa Gopalan, R.; Kulkarni, G. U.; Bhattacharya, S. *J. Mol. Struct.* **2002**, *616*, 103.

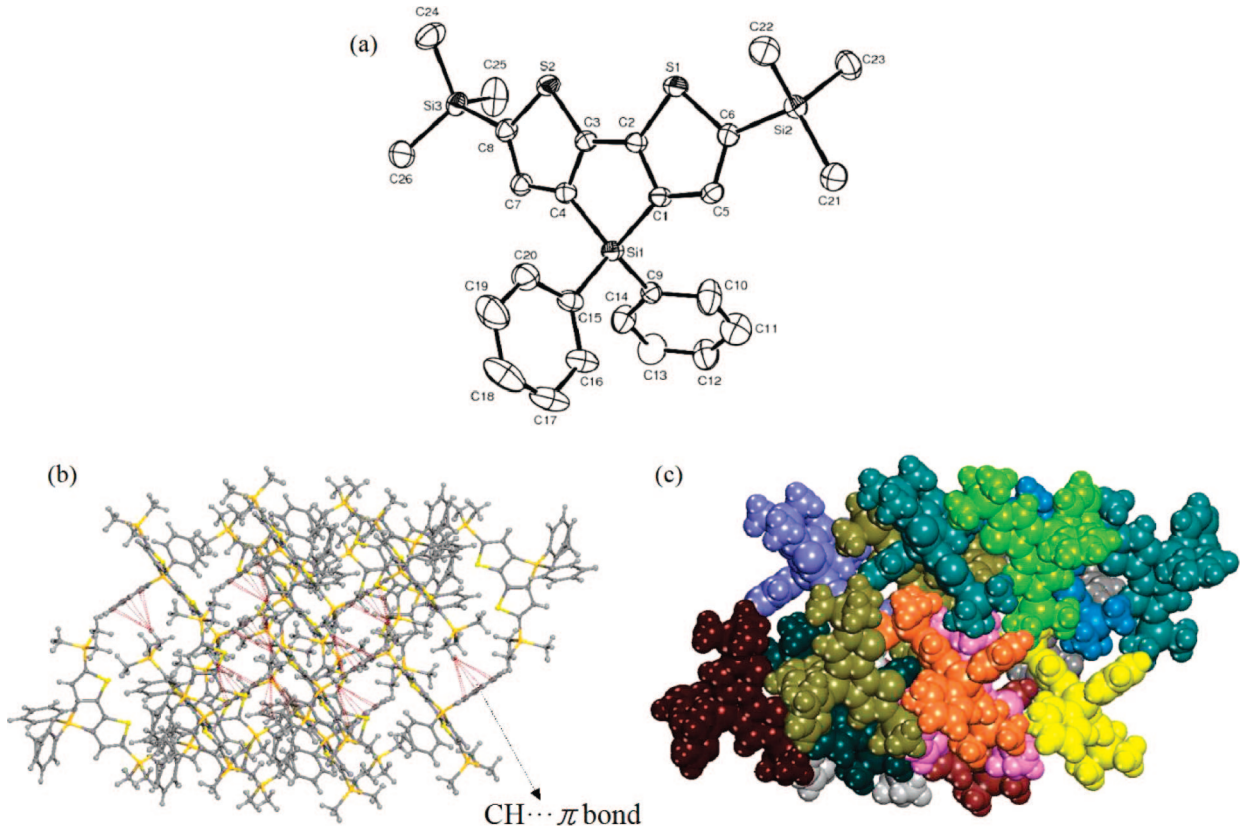

Figure 3. ORTEP drawing (30% probability thermal ellipsoids) of **2Ph-TMS**. One carbon atom (C13) in the phenyl ring was disordered over two positions. The disordered atom was refined isotropically to avoid unusual displacement parameters and is shown by a circle in the diagram. Hydrogen atoms have been omitted for clarity. Crystal packing structure (b) and space-filling diagram (c) of **2Ph-TMS**.

Table 1. Crystal Data and Structure Refinement for 3b, 2Ph-TMS, and 5

	3b	**2Ph-**TMS	**5**
empirical formula	$C_{18}H_{26}S_2Si_3$	$C_{26}H_{30}S_2Si_3$	$C_{52}H_{34}Br_2N_2S_2 \cdot C_8O_2$(THF)
fw	390.79	490.90	1054.96
temperature	293(2) K	293(2) K	293(2) K
wavelength	0.71073 Å	0.71073 Å	0.71073 Å
cryst syst, space group	monoclinic, *C*2/*c*	monoclinic, $P2_1/c$	monoclinic, $P2_1/n$
unit cell dimens	a = 21.6906(15) Å, α = 90°	a = 20.6876(16) Å, α = 90°	a = 15.261(17) Å, α = 90°
	b = 21.2005(15) Å, β = 90.325(2)°	b = 11.1624(9) Å, β = 105.098(2)°	b = 10.994(12) Å, β = 95.81(2)°
	c = 19.9077(14) Å, γ = 90°	c = 12.8583(10) Å, γ = 90°	c = 15.901(17) Å, γ = 90°
volume	9154.4(11) Å^3	2807.0(7) Å^3	2654(5) Å^3
Z, calcd density	8, 1.134 mg/m^3	4, 1.162 mg/m^3	2, 1.320 mg/m^3
μ	0.388 mm^{-1}	0.329 mm^{-1}	1.649 mm^{-1}
F(000)	3328	1040	1084
cryst size	0.32 × 0.20 × 0.19 mm	0.41 × 0.35 × 0.22 mm	0.12 × 0.29 × 0.07 mm
θ range for data collection	1.33 to 28.43°	2.06 to 28.46°	1.76 to 28.31°
limiting indices	$-28 \le h \le 29$, $-28 \le k \le 28$, $-26 \le l \le 26$	$-27 \le h \le 27$, $-14 \le k \le 14$, $-16 \le l \le 17$	$-13 \le h \le 20$, $-14 \le k \le 14$, $-20 \le l \le 21$
no. of reflns collected/unique	47 043/11 469 [R(int) = 0.0523]	28 366/7014 [R(int) = 0.0812]	17 919/6511 [R(int) = 0.1936]
max. and min. transmn	0.9311 and 0.8870	0.9311 and 0.8768	0.8933 and 0.6462
completeness to θ = 28.43	99.4%	98.9%	98.5%
refinement method	full-matrix least-squares on F^2	full-matrix least-squares on F^2	full-matrix least-squares on F^2
no. of data/restraints/params	11 469/0/412	7014/0/290	6511/0/308
goodness-of-fit on F^2	1.019	1.054	0.846
final R indices [$I > 2\sigma(I)$][a,b]	R_1 = 0.0585, wR_2 = 0.1476	R_1 = 0.0552, wR_2 = 0.1317	R_1 = 0.0773, wR_2 = 0.1760
R indices (all data)	R_1 = 0.1241, wR_2 = 0.1929	R_1 = 0.1298, wR_2 = 0.1772	R_1 = 0.2755, wR_2 = 0.2940
largest diff peak and hole	0.597 and −0.457 e Å^{-3}	0.375 and −0.336 e Å^{-3}	0.602 and −0.404 e Å^{-3}

[a] $R_1 = \sum||F_o| - |F_c|| / \sum|F_o|$ (based on reflections with $F_o^2 > 2\sigma F^2$. [b] $wR_2 = [\sum[w(F_o^2 - F_c^2)^2]/\sum[w(F_o^2)^2]]^{1/2}$; $w = 1/[\sigma^2(F_o^2) + (0.095P)^2]$; $P = [\max(F_o^2, 0) + 2F_c^2]/3$(also with $F_o^2 > 2\sigma F$.

with the UV and PL data of the dithieno-spiro-siloles (**3**), **6** exhibited a red shift of about 80 nm for the UV spectrum and 100 nm for the PL spectrum in solution (Table 3). In contrast to **3**, however, the UV and PL data of **6** varied to only a small degree as a function of ring size due to the extended conjugation in these molecules. The PL quantum yields in solution of **3** and **6** (Φ_f = 74−83% for **3** and 37−43% for **6**) show that these compounds are highly efficient fluorescent emitters.

Electrochemistry. To determine the HOMO and LUMO levels, cyclic voltammograms (CVs) were measured in CH_2Cl_2 containing 0.1 M tetrabutylammonium perchlorate (TBAP). All the dithieno-spiro-siloles (**3**) exhibited irreversible oxidation.

Table 2. Selected Bond Lengths and Angles of 3b and 2Ph-TMS

length (Å)/angle (deg)	3b	2Ph-TMS	angle (deg)	3b	2Ph-TMS
Si1−C1	1.872(3)	1.864(3)	C3−C2−C1	131.8(3)	116.8(3)
Si1−C4	1.870(4)	1.867(3)	C4−Si1−C1	91.7(2)	92.0(1)
C1−C2	1.376(5)	1.377(4)	C12−Si1−C9/C15−Si1−C9*	95.8(3)	110.7(2)*
C2−C3	1.449(4)	1.452(4)	C4−C3−C2−S1	177.8(3)	−179.6(3)
C3−C4	1.371(5)	1.371(4)	C1−C2−C3−S2	−174.1(3)	−176.1(2)
Si1−C12/Si1-C15*	1.872(4)	1.854(3)*	C2−C3−C4−C7	−175.4(3)	−178.2(3)
Si1−C9	1.861(5)	1.853(3)	C3−C2−C1−C5	176.1(3)	179.3(3)
Si1−C1−C2	107.5(2)	107.2(2)	C1−C2−C3−C4	1.2(4)	1.0(4)
Si1−C4−C3	107.2(2)	107.5(2)	Si1−C1−C2−C3	−3.6(4)	−2.5(3)
C4−C3−C2	117.2(3)	116.5(3)	Si1−C4−C3−C2	178.0(2)	1.0(3)

Table 3. UV−Vis, PL, and Thermal Data for Dithienosiloles

		PL (nm)			
dithienosilole	UV−vis (nm)[a]	solution[a]	film[b]	Φ_f (%)[c]	mp (°C)
3a	366	440	438	79	101
3b	360	428	426	74	150
3c	358	425	423	83	128
3d	353	421	421	77	135
2Ph-TMS	360	425	426	95	160
6b	443	522	534	37	255
6c	445	520	542	43	256
6d	441	515	530	40	267
2Ph-NPB	442	522	531	25	245

[a] In chloroform. [b] Emission maximum for thin solid film. [c] Relative to 9,10-diphenylanthracene in chloroform at ambient temperature.

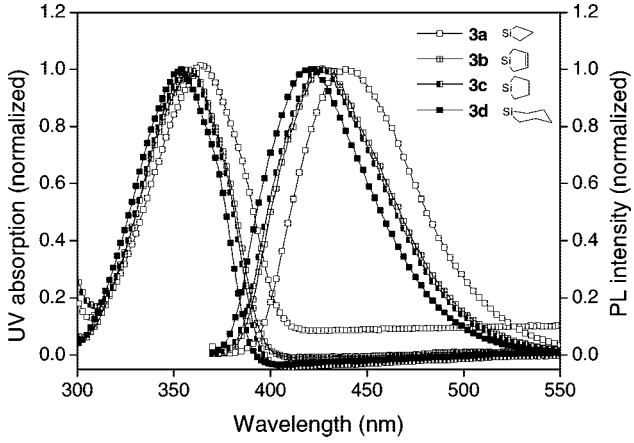

Figure 4. UV−vis absorption and PL spectra of dithienosiloles (**3**) in chloroform.

Similar to the bis(diarylamino)dithienosilole complex,[5] CVs of **6** showed no reversible peaks arising from the reduction potential but a redox peak arising from oxidation at 0.27 V, which is due to the (*N*-1-naphthyl-*N*-phenylamino)-1-phenyl moiety (Figure 7). The CV data, which were calibrated using ferrocene (4.8 eV below the vacuum level)[10] as a standard, are listed in Table 4. From the first oxidation, the HOMO energy levels of the dithieno-spiro-siloles were estimated to be from ca. −5.40 to ca. −5.45 for **3** and from ca. −4.86 to ca. −5.00 eV for **6**, respectively. Unfortunately, no reduction peaks were detected in the potential range studied. Therefore, the LUMO energy levels of the dithieno-spiro-siloles were determined from the onset of the UV−vis absorption spectra; the estimated values were ca. −2.23 to ca. −2.38 for **3** and ca. −2.41 to ca. −2.53 eV for **6**. These results show that the LUMO levels of the nonconjugated dithieno-spiro-siloles (**3**) increase as the size of the silacycloalkyl ring increases, in agreement with the blue shift in the UV spectra (Figure S6). However, due to small variations in the experimentally estimated LUMO data, this trend is not notable. By contrast, the LUMO levels of **6** vary inconsistently, as observed in the UV data. The HOMO levels of the dithieno-spiro-siloles are almost the same for all molecules in the series.

Time-of-Flight Measurements.[11] The double logarithmic plots to determine the transit time (t_τ) are illustrated in Figure 8. The optical densities of **6b** and **2Ph-NPB** films were 18726 and 18832 cm^{-1} at a wavelength of 350 nm from the N_2 laser, and the applied fields were 53 and 59 MV/m, respectively. Figure 9 shows electric field dependence of hole mobilities for two dithienosiloles, **6b** and **2Ph-NPB**. The hole mobilities were calculated using the relation $\mu = d^2/V \times t_r$, where d and V are the sample thickness and applied voltage. As expected, the result

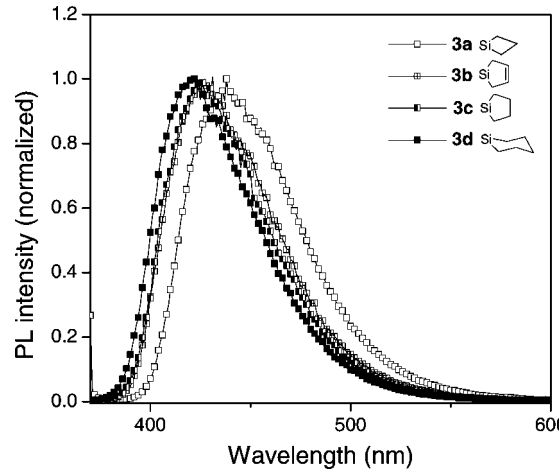

Figure 5. PL spectra of dithienosiloles (**3**) in a solid film.

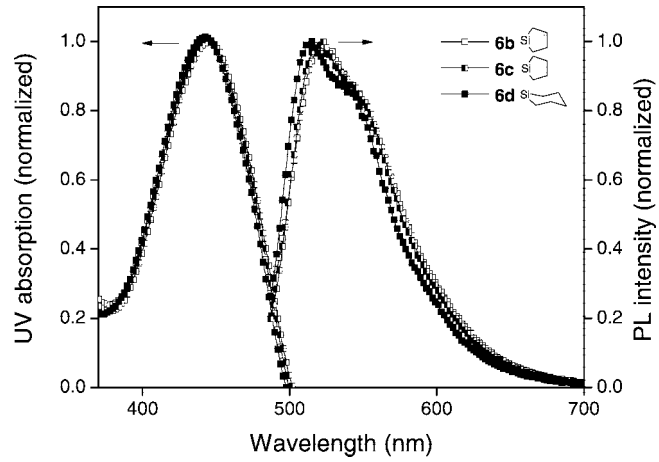

Figure 6. UV−vis absorption and PL spectra of dithienosiloles (**6**) in chloroform.

(10) Ferman, J.; Kakareka, J. P.; Klooster, W. T.; Mullin, J. L.; Quattrucci, J.; Ricci, J. S.; Tracy, H. J.; Vining, W. J.; Wallace, S. *Inorg. Chem.* **1999**, *38*, 2464.

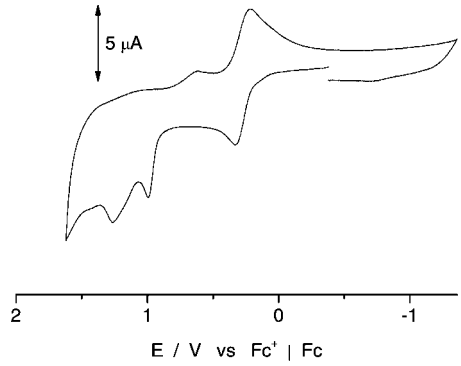

Figure 7. Cyclic voltammogram of 1 mM silacyclohexyldithienosilole (**6d**) at a platinum disk electrode; in CH_2Cl_2 containing 0.1 M Bu_4NBF_4; $v = 0.1$ V/s.

showed that **6b** has higher hole mobility values than **2Ph-NPB**, in agreement with the expectation from the dense crystal packing structure of cyclized ring systems. This suggests that a ring on a silicon atom builds an efficient charge-transport channel, resulting from the reduced intermolecular distance between adjacent dithienosilole rings.

Fabrication of OLED Devices. Unfortunately, the cyclic dithieno-spiro-siloles (**3**) could not be deposited on ITO because of its low vaporization temperature and low molecular weight. For this reason, arylamine-substituted dithienosiloles (**6** and **2Ph-NPB**) were used for the fabrication of OLED devices with the device structure of ITO/NPB/dithienosilole (**6** or **2Ph-NPB**)/BCP/Alq_3/LiF/Al (Figure 10). As shown in Figure 11 and Table 5, the device containing **6b** showed better performance, exhibiting a maximum brightness of 12 640 cd/m^2 at 10 V and a current efficiency of 3.70 cd/A at 1 mA/cm^2. In the $I-V-L$ curve, the characteristics of **6b**−**d** showed a remarkable enhancement compared with that of **2Ph-NPB**. The turn-on voltages were 2.2−2.8 V for **6b**−**d** and 4.3 V for **2Ph-NPB** ($I-V$), and the luminances were 1184−4288 cd/m^2 for **6b**−**d** and 41 cd/m^2 for **2Ph-NPB** ($L-V$) at 6 V. These results demonstrate that the cyclization of a silanylene unit in the dithienosiloles has positive effects on the EL properties of the molecules. The PL and EL spectra of each device were almost identical, indicating that the emissions originated from the layer of **6** in the OLED device structure (Table 5).

Conclusions

A series of new types of 1,1-silacycloalkyl-substituted dithieno-spiro-siloles were synthesized, and the corresponding photophysical properties were measured. From the crystal packing, it was observed that **3b** exhibited a smaller intermolecular distance compared to **2Ph-TMS**. Cyclized **6b** showed higher hole mobility than the acyclic analogue **2Ph-NPB** on the basis of time-of-flight. This improved carrier-transporting mobility gave rise to promising results when the compounds were used as the emission layers in OLEDs: the $I-V$ and $L-V$ curves showed that the devices containing cyclic-silanylene dithieno-spiro-siloles (**6b**−**d**), which have a crossed-blade configuration, had driving voltages lower than that of the device based on **2Ph-NPB**. In addition, the dithieno-spiro-siloles (**3**) showed intensified expansion of the band gap as the size of the exocyclic ring was increased, whereas the band gap of the conjugated bis(diarylamino)dithieno-spiro-siloles (**6**) was insensitive to the ring size. The present results demonstrate that cyclization on a silanylene unit improved structural organization in crystal packing and reinforced charge-carrier mobility in the solid state, thereby enabling the fabrication of high-performance EL devices.

Experimental Section

General Procedures. All manipulations were performed under dry nitrogen (or an argon atmosphere) using standard Schlenk techniques. THF was dried over sodium/benzophenone. ^{1}H and ^{13}C spectra were recorded on a Varian Unity Inova AS600 spectrometer operating at 599.80 and 150.83 MHz, respectively. All proton and carbon chemical shifts were measured relative to internal residual benzene from the lock solvent (99.9% $CDCl_3$) and then referenced to Me_4Si (0.00 ppm). The elemental analyses were performed with a Carlo Erba Instruments CHNS-O EA 1108 analyzer. High-resolution tandem mass spectrometry (JEOL LTD JMS-700) was performed by the Korean Basic Science Institute (Seoul). Absorption and photoluminescence spectra were recorded on a Shimadzu UV-3101PC UV−vis−NIR scanning spectrophotometer and a Varian Cary Eclipse fluorescence spectrophotometer, respectively. The fluorescence quantum yields in chloroform using 9,10-diphenylanthracene as a standard were determined by the dilution method. Cyclic voltammetry (CV) experiments were performed using a BAS 100 electrochemical analyzer. Platinum, platinum wire, and Ag/$AgNO_3$ (0.10 M) were used as the working, counter, and reference electrodes, respectively. The CV experiments were performed using these three electrodes immersed in a solution of 0.1 M tetrabutylammonium perchlorate (Bu_4NClO_4) in anhydrous CH_2Cl_2 at room temperature under argon with a scan rate of 0.1 V/s. The hole mobilities of two dithienosiloles (**6b** and **2Ph-NPB**) were measured with thick sandwiched samples (1.5 and 3.4 μm, respectively) using ITO and Al electrodes. Devices with the structure ITO/dithienosilole/Al (100 nm) were fabricated for the TOF measurements. The sample area was 2 × 2 mm^2. The sample was irradiated with a N_2 laser (Photon Technology International Inc. GL 3300) with a pulse width of 10 nm at a wavelength of 350 nm. A resistor was connected in series to the samples, an electric field was biased to the sample and the resistor, and the photocurrent was measured with a digital oscilloscope (Lecroy LC564A). 2,2′-Bithiophene, *N*-phenyl-1-naphthylamine, and aluminum oxide (neutral) for column chromatography were purchased from Aldrich and used without further purification. Silacyclobutyl dichloride (**1a**), silacyclopentenyl dichloride (**1b**), silacyclopentyl dichloride (**1c**), and silacyclohexyl dichloride (**1d**) were all prepared according to the literature method.[12] 3,3′-Dibromo-5,5′-bis(trimethylsilyl)-2,2′-bithiophene and 1,1-diphenyl-5,5′-bis(trimethylsilyl)dithienosiloles were also synthesized by methods reported in the literature.[2h]

Synthesis of 5,5′-Bis(trimethylsilyl)dithieno-spiro-silole (3a). To a stirred solution of 3,3′-dibromo-5,5′-bis(trimethylsilyl)-2,2′-bithiophene (4.68 g, 10 mmol) in THF (100 mL) was added a solution of 2.5 M *n*-BuLi/hexane (8.8 mL, 22 mmol) at −78 °C, and the resulting mixture was stirred at the same temperature for 1 h. Then, 3.0 mL (11 mmol) of silacyclobutyl dichloride (**1a**) was added and the mixture was stirred at room temperature for 6 h. After filtering the resulting mixture through a pad of Celite, the volatile solvent was removed under reduced pressure and the residue was purified by flash chromatography over silica gel using hexane as the eluent. Recrystallization from hexane at 0 °C afforded **3a** as a white powder. Yield: 2.05 g (54%). Mp: 100−102 °C. ^{1}H NMR

(11) Melnyk, A. R.; Pai, D. M. In *Determination of Electronic and Optical Properties, Physical Methods of Chemistry Series*, 2nd ed.; Rossiter, B. C., Baetzold, R. C., Eds.; Wiley: New York, Vol. VIII,1993.

(12) Kim, S.-J.; Jung, I. N.; Yoo, B. R.; Cho, S.; Ko, J.; Kim, S. H.; Byun, D.; Kang, S. O. *Organometallics* **2001**, *20*, 2136.

(13) (a) *SMART* and *SAINT*; Bruker Analytical X-Ray Division: Madison, WI, 2002. (b) Sheldrick, G. M. *SHELXTL-PLUS Software Package*; Bruker Analytical X-Ray Division: Madison, WI, 2002.

Table 4. Oxidation and Reduction Potentials of Dithienosiloles

	oxidation [V][a]									
dithienosilole	E_{pa1} [V]	E_{pa2} [V]	E_{pa3} [V]	E_{pc1} [V]	E_{pc2} [V]	$E^{0\prime}$[b]	E_{onset}^{ox} [V]	E_g^{opt} [eV] [c]	HOMO [eV] [d]	LUMO [eV][d]
3a	0.74	1.2					0.65	3.07	−5.45	−2.38
3b	0.72	1.31					0.64	3.14	−5.44	−2.30
3c	0.72	1.11					0.60	3.15	−5.40	−2.25
3d	0.70	0.92					0.63	3.20	−5.43	−2.23
2Ph-TMS	0.77						0.70	3.15	−5.50	−2.35
6b	0.16	0.29	0.93	0.12	0.21	0.14, 0.25	0.06	2.45	−4.86	−2.41
6c	0.33	1.01	1.29	0.22		0.28	0.19	2.46	−4.99	−2.53
6d	0.32	0.99	1.26	0.21		0.27	0.20	2.48	−5.00	−2.52
2Ph-NPB	0.18	0.31	1.01	0.14	0.25	0.16, 0.28	0.08	2.45	−4.88	−2.43

[a] E_{pa} = anodic peak potential; E_{pc} = cathodic peak potential; E_{onset} = onset potential. [b] $E^{0\prime} = (E_{pc} + E_{pa})/2$. [c] Optical bandgap E_g^{opt} from the absorption edge. [d] HOMO and LUMO levels were determined using the following equations: E_{HOMO} (eV) = $-e(E_{onset}^{ox} + 4.8)$, E_{LUMO} (eV) = $-e(E_{HOMO} - E_g^{opt})$.

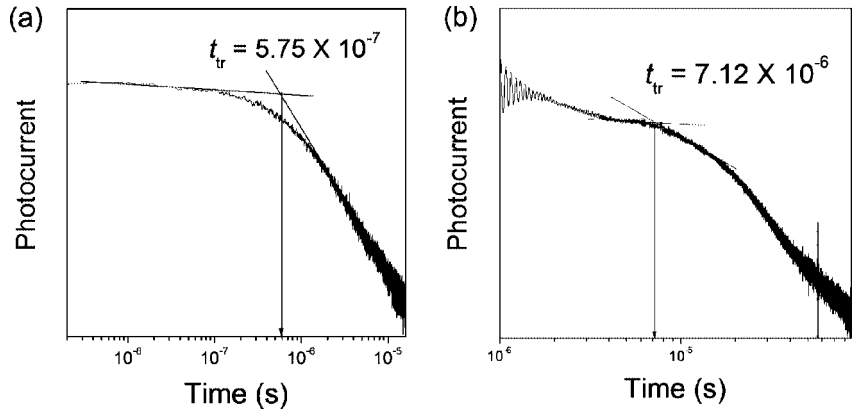

Figure 8. Double logarithmic plots of transient photocurrent at room temperature. ITO/**6b** (1.5 μm) or **2Ph-NPB** (3.4 μm)/Al. (a) **6b**. (b) **2Ph-NPB**.

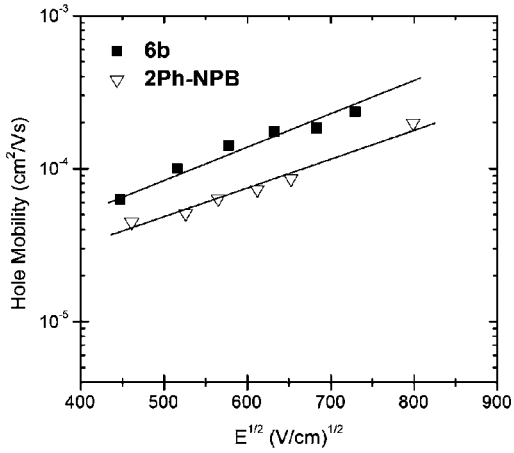

Figure 9. Electrical field dependence of carrier mobilities for two dithienosiloles (**6b** vs **2Ph-NPB**).

($CDCl_3$): δ 7.28 (s, 2H, thiophene ring protons), 2.38 (m, 2H, $SiCH_2CH_2$, $^3J_{H-H}$ = 8.4 Hz), 1.57 (t, 4H, $SiCH_2CH_2$, $^3J_{H-H}$ = 8.4 Hz), 0.34 (s, 18H, Me_3Si). ^{13}C NMR ($CDCl_3$): δ 155.13, 142.03, 141.59, 136.33, 18.83 ($SiCH_2CH_2$), 15.23 ($SiCH_2CH_2$), 0.00 ($SiMe_3$). FAB-MS: calcd for $[C_{17}H_{26}S_2Si_3]^+$ 378.1, found 378.04. Anal. Calcd for $C_{17}H_{26}S_2Si_3$: C, 53.91; H, 6.92. Found: C, 53.82; H, 6.89.

Synthesis of 5,5′-Bis(trimethylsilyl)dithieno-spiro-silole (3b). This compound was prepared by a procedure similar to that used for **3a**, but using silacyclopentenyl dichloride (**1b**) instead of silacyclobutyl dichloride (**1a**); the product (**3b**) was isolated as a crystalline, white solid. Yield: 2.15 g (55%). Mp: 150−152 °C. ^{1}H NMR ($CDCl_3$): δ 7.21 (s, 2H, thiophene ring protons), 6.16 (s, 2H, $SiCH_2CH$), 1.75 (s, 4H, $SiCH_2CH$), 0.35 (s, 18H, Me_3Si). ^{13}C NMR ($CDCl_3$): δ 155.34, 142.21, 141.96, 136.39, 131.44 ($SiCH_2CH$), 13.99 ($SiCH_2CH$), 0.09 ($SiMe_3$). FAB-MS: calcd for $[C_{18}H_{26}S_2Si_3]^+$ 390.1, found 390.05. Anal. Calcd for $C_{18}H_{26}S_2Si_3$: C, 55.32; H, 6.71. Found: C, 55.29; H, 6.68.

Synthesis of 5,5′-Bis(trimethylsilyl)dithieno-spiro-silole (3c). This compound was prepared by a procedure similar to that used for **3a**, but using silacyclopentyl dichloride (**1c**) instead of silacyclobutyl dichloride (**1a**); the product (**3c**) was isolated as a crystalline, green solid. Yield: 2.04 g (52%). Mp: 126−128 °C. ^{1}H NMR ($CDCl_3$): δ 7.16 (s, 2H, thiophene ring protons), 1.87 (m, 4H, $SiCH_2CH_2$, $^3J_{H-H}$ = 13.8 Hz), 1.00 (t, 4H, $SiCH_2CH_2$, $^3J_{H-H}$ = 7.2 Hz), 0.34 (s, 18H, Me_3Si). ^{13}C NMR ($CDCl_3$): δ 154.96, 143.12, 141.73, 136.27, 27.42 ($SiCH_2CH_2$), 9.69 ($SiCH_2CH_2$), 0.11 ($SiMe_3$). FAB-MS: calcd for $[C_{18}H_{28}S_2Si_3]^+$ 392.1, found 392.07. Anal. Calcd for $C_{18}H_{28}S_2Si_3$: C, 55.04; H, 7.18. Found: C, 55.03; H, 7.15.

Synthesis of 5,5′-Bis(trimethylsilyl)dithieno-spiro-silole (3d). This compound was prepared by a procedure similar to that used for **3a**, but using silacyclohexyl dichloride (**1d**) instead of silacyclobutyl dichloride (**1a**); the product (**3d**) was isolated as a greenish-blue solid. Yield: 1.91 g (47%). Mp: 133−135 °C. ^{1}H NMR ($CDCl_3$): δ 7.22 (s, 2H, thiophene ring protons), 1.97 (m, 4H, $SiCH_2CH_2CH_2$), 1.63 (m, 2H, $SiCH_2CH_2CH_2$), 0.94 (t, 4H, $SiCH_2CH_2CH_2$, $^3J_{H-H}$ = 10.2 Hz), 0.34 (s, 18H, Me_3Si). ^{13}C NMR ($CDCl_3$): δ 154.93, 143.84, 141.52, 136.71, 30.03 ($SiCH_2CH_2CH_2$), 25.95 ($SiCH_2CH_2CH_2$), 11.74 ($SiCH_2CH_2CH_2$), 0.53 (Me_3Si). FAB-MS: calcd for $[C_{19}H_{30}S_2Si_3]^+$ 406.1, found 406.08. Anal. Calcd for $C_{19}H_{30}S_2Si_3$: C, 56.09; H, 7.43. Found: C, 56.05; H, 7.42.

Synthesis of 3,3′-Dibromo-5,5′-bis[(*N*-1-naphthyl-*N*-phenylamino)-1-phenyl]-2,2′-dithiophene (5). To a mixture of aryl boronic acids (**4**) (6.78 g, 20 mmol), 3,3′,5,5′-tetrabromobithiophene (4.33 g, 9 mmol), and $Pd(PPh_3)_4$ (1.16 g, 5 mol %) were added degassed 0.2 M K_2CO_3 (100 mL, 20 mmol) and THF (100 mL). The resulting yellow solution was refluxed for 6 h. The organic

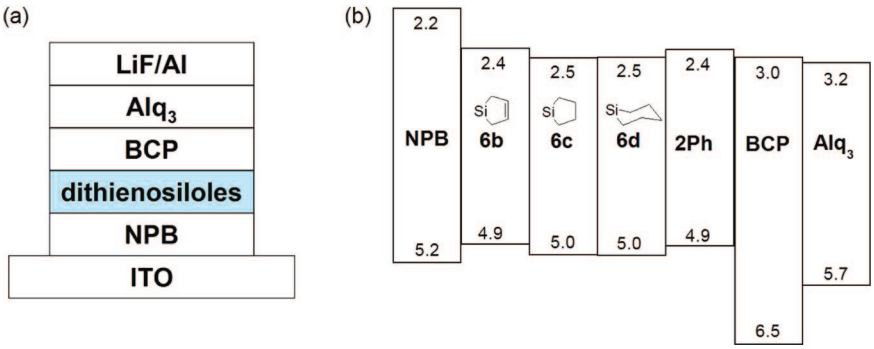

Figure 10. Diagrams showing the device structure (a) and HOMO−LUMO levels (b) estimated by CVs and UV absorption.

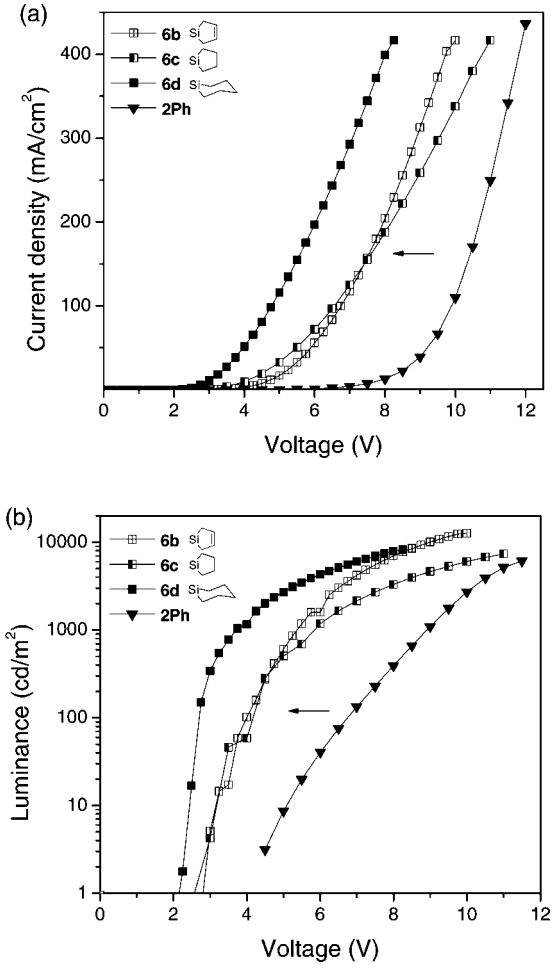

Figure 11. (a) Current density vs voltage ($I-V$) and (b) luminance vs voltage ($L-V$) for the devices using **6** or **2Ph-NPB** as an emitting layer.

layer was extracted with CH_2Cl_2 and dried over anhydrous $MgSO_4$. The volatile solvent was then removed under reduced pressure, and the residue was purified by flash chromatography over silica gel using ethylacetate/hexane (v/v = 1:10) as the eluent. The product **5** was obtained as a yellow powder. Yield: 7.29 g (89%). ^{1}H NMR ($CDCl_3$): δ 7.93 (t, 2H, *Ph*, $^3J_{H-H}$ = 7.8 Hz), 7.82 (d, 2H, *Ph*, $^3J_{H-H}$ = 8.1 Hz), 7.50 (m, 6H, *Ph*), 7.38 (m, 6H, *Ph*), 7.25 (m, 6H, *Ph*), 7.13 (m, 6H, *Ph*), 6.99 (m, 6H, *Ph*). ^{13}C NMR ($CDCl_3$): δ 148.92, 147.77, 145.59, 143.04, 135.43, 131.25, 129.90, 129.01, 128.72, 127.78, 127.02, 126.89, 126.73, 126.65, 126.29, 125.65, 124.29, 123.57, 121.69, 120.32, 112.56. FAB-MS: calcd for $[C_{52}H_{34}Br_2N_2S_2]^+$ 910.1, found 909.88. Anal. Calcd for $C_{52}H_{34}Br_2N_2S_2$: C, 68.57; H, 3.76. Found: C, 68.54; H, 3.79.

Synthesis of 5,5′-Bis[(*N*-1-naphthyl-*N*-phenylamino)-1-phenyl]-2,2′-dithieno-spiro-silole (6b). To a stirred solution of 3,3′-dibromo-5,5′-bis[(*N*-1-naphthyl-*N*-phenylamino)-1-phenyl]-2,2′-dithiophene (1.82 g, 2 mmol) in THF (30 mL) was added 1.6 mL (4 mmol) of *n*-BuLi (2.5 M in hexane) at −78 °C, and the resulting mixture was stirred at the same temperature for 1 h. Then, 0.321 g (2.1 mmol) of silacyclopentenyl dichloride (**1b**) was slowly added, after which the mixture was warmed to room temperature and stirred for 6 h. The mixture was then hydrolyzed with water, and the organic layer was extracted with CH_2Cl_2 and dried over $MgSO_4$. The volatile solvent was removed under reduced pressure, and the residue was purified by alumina column chromatography using ethylacetate/hexane (v/v = 1:5) as the eluent. Recrystallization from toluene at 0 °C produced **6b** as an orange powder. Yield: 1.05 g (63%). Mp: 255 °C. ^{1}H NMR ($CDCl_3$): δ 7.92 (d, 2H, *Ph*, $^3J_{H-H}$ = 9.0 Hz), 7.88 (d, 2H, *Ph*, $^3J_{H-H}$ = 7.8 Hz), 7.77 (d, 2H, *Ph*, $^3J_{H-H}$ = 8.4 Hz), 7.45 (m, 4H, *Ph*), 7.37 (m, 4H, *Ph*), 7.34 (m, 6H, *Ph*), 7.20 (m, 4H, *Ph*), 7.15 (m, 2H, thiophene ring protons), 7.07 (m, 4H, *Ph*), 6.96 (m, 4H, *Ph*), 6.13 (s, 2H, $SiCH_2CH$), 1.73 (s, 4H, $SiCH_2CH$). ^{13}C NMR ($CDCl_3$): δ 148.36, 147.94, 147.64, 145.60, 143.11, 140.70, 135.24, 131.40 ($SiCH_2CH$), 131.11, 129.17, 128.41, 127.61, 127.23, 126.63, 126.49, 126.35, 126.28, 126.19, 124.29, 124.14, 122.32, 121.45, 13.94 ($SiCH_2CH$). FAB-MS: calcd for $[C_{56}H_{40}N_2S_2Si]^+$ 832.2, found 832.03. Anal. Calcd for $C_{56}H_{40}N_2S_2Si$: C, 80.73; H, 4.84. Found: C, 80.69; H, 4.82.

Synthesis of 5,5′-Bis[(*N*-1-naphthyl-*N*-phenylamino)-1-phenyl]-2,2′-dithieno-spiro-silole (6c). This compound was prepared by a procedure similar to that used for **6b**, but using silacyclopentyl dichloride (**1c**) instead of silacyclopentenyl dichloride (**1b**); the product (**6c**) was isolated as a crystalline, orange solid. Yield: 1.19 g (71%). Mp: 256 °C. ^{1}H NMR ($CDCl_3$): δ 7.94 (d, 2H, *Ph*, $^3J_{H-H}$ = 9.0 Hz), 7.90 (d, 2H, *Ph*, $^3J_{H-H}$ = 8.4 Hz), 7.80 (d, 2H, *Ph*, $^3J_{H-H}$ = 8.4 Hz), 7.48 (m, 4H, *Ph*), 7.40 (m, 4H, *Ph*), 7.36 (m, 6H, *Ph*), 7.23 (m, 4H, *Ph*), 7.15 (m, 2H, thiophene ring protons), 7.09 (m, 4H, *Ph*), 6.99 (m, 4H, *Ph*), 1.87 (m, 4H, $SiCH_2CH_2$), 1.02 (m, 4H, $SiCH_2CH_2$). ^{13}C NMR ($CDCl_3$): δ 148.15, 148.14, 147.85, 143.33, 143.12, 135.99, 135.50, 131.37, 129.42, 128.66, 127.51, 127.35, 126.87, 126.74, 126.61, 126.44, 124.41, 122.65, 122.55, 121.76, 121.57, 27.67 ($SiCH_2CH_2$), 9.89 ($SiCH_2CH_2$). FAB-MS: calcd for $[C_{56}H_{42}N_2S_2Si]^+$ 834.3, found 834.13. Anal. Calcd for $C_{56}H_{42}N_2S_2Si$: C, 80.54; H, 5.07. Found: C, 80.50; H, 5.06.

Synthesis of 5,5′-Bis[(*N*-1-naphthyl-*N*-phenylamino)-1-phenyl]-2,2′-dithieno-spiro-silole (6d). This compound was prepared by a procedure similar to that used for **6b**, but using silacyclohexyl dichloride (**1d**) instead of silacyclopentenyl dichloride (**1b**); the product (**6d**) was isolated as an orange solid. Yield: 1.15 g (68%). Mp: 267 °C. ^{1}H NMR ($CDCl_3$): δ 7.92 (d, 2H, *Ph*, $^3J_{H-H}$ = 8.4 Hz), 7.88 (d, 2H, *Ph*, $^3J_{H-H}$ = 7.8 Hz), 7.77 (d, 2H, *Ph*, $^3J_{H-H}$ = 7.8 Hz), 7.46 (m, 4H, *Ph*), 7.40 (m, 4H, *Ph*), 7.35 (m, 6H, *Ph*), 7.20 (m, 6H, *Ph*), 7.07 (m, 4H, *Ph*), 6.96 (m, 4H, *Ph*), 1.96 (m, 4H, $SiCH_2CH_2CH_2CH_2$), 1.62 (m, 2H, $SiCH_2CH_2CH_2CH_2$), 0.95 (t, 4H, $SiCH_2CH_2CH_2CH_2$, $^3J_{H-H}$ = 6.6 Hz). ^{13}C NMR ($CDCl_3$): δ 147.99,

Table 5. EL Spectra Data and Performance Characteristics of Devices[a]

dithienosilole	CIE coordinates (x, y)	EL emission λ_{max} (nm)[b]	luminance (cd/m^2) @6 V	max. luminance (cd/m^2)	max. current efficiency (cd/A)	turn-on voltage (V)[c]
6b[a]	(0.40, 0.57)	530, 555	1595	12640(10V)	3.70	2.8
6c[a]	(0.40, 0.57)	533, 556	1184	7362(11V)	1.72	2.5
6d[a]	(0.37, 0.60)	525, 548	4288	8204(8.3V)	3.11	2.2
2Ph-NPB[a]	(0.40, 0.57)	531, 557	41	6000(11.5V)	3.05	4.3

[a] Device structure: ITO/NPB (50 nm)/dithienosilole (40 nm)/BCP (5 nm)/Alq_3 (5 nm)/LiF (0.5 nm)/Al (100 nm). [b] Determined from the EL spectra (Figure 12). [c] Defined as the voltage required to give a brightness of 1 cd/m^2.

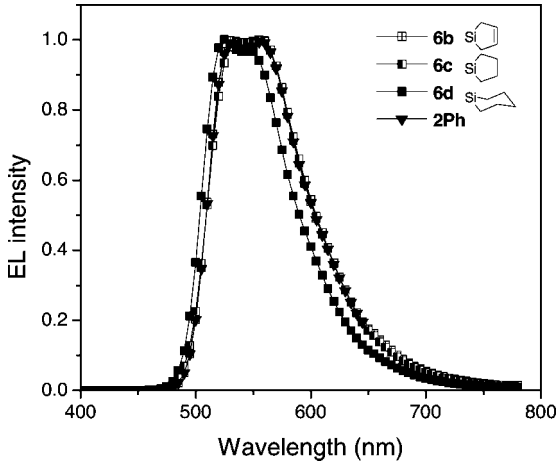

Figure 12. EL spectra of the devices based on the silacycloalkyl dithienosiloles (**6**).

147.86, 147.56, 145.16, 143.16, 142.26, 135.25, 131.11, 129.16, 128.41, 127.79, 127.21, 126.60, 126.47, 126.35, 126.18, 124.63, 124.16, 122.28, 122.08, 121.53, 29.58 ($SiCH_2CH_2CH_2$), 25.52 ($SiCH_2CH_2CH_2$), 11.19 ($SiCH_2CH_2CH_2$). FAB-MS: calcd for $[C_{57}H_{44}N_2S_2Si]^+$ 848.3, found 848.07. Anal. Calcd for $C_{57}H_{44}N_2S_2Si$: C, 80.62; H, 5.22. Found: C, 80.59; H, 5.21.

Synthesis of 1,1-Diphenyl-5,5′-bis[(*N*-1-naphthyl-*N*-phenylamino)-1-phenyl]-2,2′-dithienosilole (2Ph-NPB). This compound was prepared by a procedure similar to that used for **6b**, but using diphenyl dichloride instead of silacyclopentenyl dichloride (**1b**); the product (**2Ph-NPB**) was isolated as an orange solid. Yield: 1.40 g (75%). Mp: 245 °C. ^{1}H NMR ($CDCl_3$): δ 7.94 (d, 2H, *Ph*, $^3J_{H-H}$ = 8.4 Hz), 7.91 (d, 2H, *Ph*, $^3J_{H-H}$ = 8.4 Hz), 7.79 (d, 2H, *Ph*, $^3J_{H-H}$ = 8.4 Hz), 7.69 (d, 4H, *Ph*, $^3J_{H-H}$ = 7.8 Hz), 7.48 (m, 4H, *Ph*), 7.44 (m, 4H, *Ph*), 7.37 (m, 6H, *Ph*), 7.33 (m, 6H, *Ph*), 7.24 (m, 4H, *Ph*), 7.09 (m, 4H, *Ph*), 6.99 (m, 6H, *Ph*). ^{13}C NMR ($CDCl_3$): δ 148.66, 147.95, 147.69, 145.87, 143.12, 140.51, 135.44, 135.24, 131.67, 131.09, 130.32, 129.17, 128.41, 128.18, 127.59, 127.20, 126.62, 126.48, 126.33, 126.18, 124.48, 124.14, 122.34, 122.14, 121.48. FAB-MS: calcd for $[C_{64}H_{44}N_2S_2Si]^+$ 932.27, found 932.11. Anal. Calcd for $C_{64}H_{44}N_2S_2Si$: C, 82.37; H, 4.75. Found: C, 82.32; H, 4.72.

Crystal Structure Determination. Crystals of **3b**, **2Ph-TMS**, and **5** were obtained from EtOH/hexane (v/v = 1:20), hexane, and ethylacetate/hexane (v/v = 1:30), respectively, and mounted on the diffractometer. Preliminary examination and data collection were performed using a Bruker SMART CCD detector system single-crystal X-ray diffractometer equipped with a sealed-tube X-ray source (40 kV × 50 mA) using graphite-monochromated Mo Kα radiation (λ = 0.71073 Å). Preliminary unit cell constants were determined from a set of 45 narrow-frame (0.3° in ω) scans. The double-pass method of scanning was used to exclude any noise. The collected frames were integrated using an orientation matrix determined from the narrow-frame scans. The SMART software package was used for data collection, and SAINT was used for frame integration.[13a] Final cell constants were determined by a global refinement of *xyz* centroids of reflections harvested from the entire data set. Structure solution and refinement were carried out using the SHELXTL-PLUS software package.[13b] Detailed information is listed in Table 1.

Fabrication of OLED Devices. ITO-coated glass (20 Ω/sq) was first cleaned by conventional procedures. Under an inert atmosphere in a fabrication chamber, the sample was exposed to UV/ozone treatment. Then organic and metal layers were deposited thermally onto the ITO surface at a rate of 1−2 Å/s at a pressure of ca. 4×10^{-6} Torr. Typical devices were fabricated with NPB as the hole-transporting layer (HTL, 50 nm), **6** or **2Ph-NPB** as the emitting layer (EML, 40 nm), BCP (5 nm) as the hole-blocking layer, and Alq_3 (5 nm) as the electron-transporting layer (ETL). LiF (0.5 nm) and Al (100 nm) were deposited as the cathode. The deposited film thickness was measured by a Tencor P-2 long scan profiler. The characteristics of the OLED device were measured using a Photoresearch PR650 spectrometer and Keithley 306 source measure unit.

Acknowledgment. This work was supported by a grant (no. R02-2004-000-10095-0) from the Basic Research Program of the Korea Science and Engineering Foundation.

Supporting Information Available: ^{1}H and ^{13}C NMR spectroscopic data, intermolecular distance comparison in the crystal packing structure (**3b** and **2Ph-TMS**), HOMO−LUMO levels of **3** estimated by CVs and UV absorption, and DFT calculation results. This material is available free of charge via the Internet at http://pubs.acs.org.

OM7012088